
Multirate Training of Neural Networks

Tiffany Vlaar

Department of Mathematics
University of Edinburgh
Tiffany.Vlaar@ed.ac.uk

Benedict Leimkuhler

Department of Mathematics
University of Edinburgh
B.Leimkuhler@ed.ac.uk

Abstract

We propose multirate training of neural networks: partitioning neural network parameters into “fast” and “slow” parts which are trained simultaneously using different learning rates. By choosing appropriate partitionings we can obtain large computational speed-ups for transfer learning tasks. We show that for various transfer learning applications in vision and NLP we can fine-tune deep neural networks in almost half the time, without reducing the generalization performance of the resulting model. We also discuss other splitting choices for the neural network parameters which are beneficial in enhancing generalization performance in settings where neural networks are trained from scratch. Finally, we propose an additional multirate technique which can learn different features present in the data by training the full network on different time scales simultaneously. The benefits of using this approach are illustrated for ResNet architectures on image data. Our paper unlocks the potential of using multirate techniques for neural network training and provides many starting points for future work in this area.

1 Introduction

Multirate techniques have been widely used for efficient simulation of multiscale ordinary differential equations (ODEs) and partial differential equations (PDEs) [31, 7, 8, 9, 6, 3], yet appear to have been largely overlooked for neural network training. The motivation behind using multirate techniques is usually the presence of fast and slow time-scales in the system dynamics and simulations of systems which are computationally infeasible to evolve with a single time step. This motivation does not transfer easily to the training of neural networks, which explains the limited exploration of such techniques in this area. In this article we seek to change this. We illustrate the benefit of using multirate techniques for a variety of neural network training applications.

In Figure 1 we demonstrate the effect of latent multiple time scales in deep learning applications. Here we have trained a WideResNet-16 architecture on a patch-augmented CIFAR-10 dataset [23] using SGD with momentum and weight decay and different learning rates. Some images contain both the patch and CIFAR-10 data, while other images only contain the patch or are patch-free. When training using a large learning rate, the network is unable to memorize the patch, but achieves a high accuracy on patch-free data. Meanwhile, when training using a small learning rate the network can memorize the patch quickly, but the accuracy on the clean data is lower. We also demonstrate that a multirate approach, which trains and combines the weights of two copies of the network on two different time-scales (as explained in Section 3.2), can both memorize the patch and obtain a high accuracy on the patch-free data. Multirate methods thus show potential for simultaneously gathering information present on different time-scales in the data during training.

We consider multirate training both *within* networks and *across* networks. The former partitions a neural network parameter into fast and slow, whereas the latter trains multiple copies of a network on multiple scales simultaneously. Our multirate methods are straightforward to implement and act as an add-on to existing optimization schemes; they can be combined with any desired base algorithm.

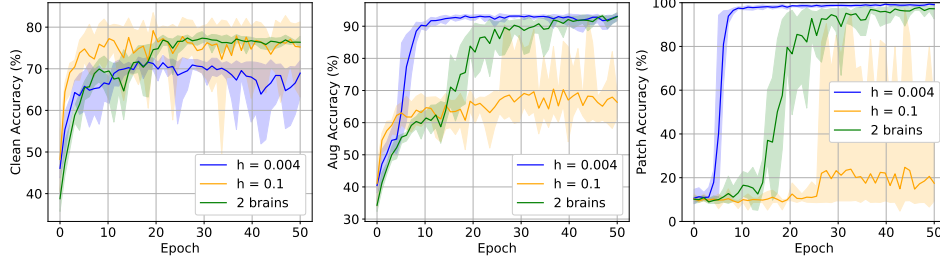


Figure 1: WideResNet-16 trained on patch-augmented CIFAR-10 [23]. Of the training data: 20% is patch-free, 16% has only the patch, and the rest has both data and patch. Left: clean validation set. Middle: augmented data with patches. Right: patch-only data. A net trained using a small learning rate (blue) learns the patch quickly, whereas a large learning rate (orange) gives higher accuracy on clean data. Our multirate method (green) trained on both timescales ($h_1 = 0.004$, $h_2 = 0.1$, see Sec. 3.2) is able to simultaneously memorize the patches and obtain high accuracy on the clean data.

Our contributions are as follows:

- We propose multirate algorithms for neural network training. We describe two distinct algorithms for this purpose. In one variant we propose linear drift of the slow parameters during the fast parameter update as a novel technique for multirate training.
- We use a multirate technique to train deep neural networks for transfer learning applications in vision and NLP in half the time, without losing much (if any) generalization performance.
- We propose a new regularization technique for the training of neural networks, which iteratively randomly selects new subsets of the neural network to form the slow parameters.
- We propose a “multi-brain” approach: using different time-scales to iteratively train and combine multiple copies (brains) of a neural network to improve generalization performance.

We conclude that multirate methods can enhance current neural network training techniques and form a promising direction for future theoretical and experimental work.

2 Background

Multirate methods use different step sizes for different parts of the system. Faster parts are integrated with smaller step sizes, while slow components are integrated using larger step sizes, which are integer multiples of the fast step size. Multirate methods have been used for more than 60 years [31] in a wide variety of areas [6, 9]. A seminal work of Gear (1974) [7] analyzed the accuracy and stability of Euler-based multirate methods applied to a system of ODEs with slow and fast components. The system of ODEs that forms the starting point for most neural network training schemes is $d\theta = G(\theta)dt$, where $\theta \in \mathbb{R}^n$ are the neural network parameters and G represents the gradient of the loss of the entire dataset. As a starting point for our multirate approach we partition the parameters as $\theta = (\theta_F, \theta_S)$, with $\theta_F \in \mathbb{R}^{n_F}$, $\theta_S \in \mathbb{R}^{n_S}$, $n = n_F + n_S$, and system of ODEs:

$$d\theta_F = G_F(\theta)dt, \quad d\theta_S = G_S(\theta)dt, \quad (1)$$

where G_F and G_S are the gradients with respect to θ_F and θ_S , resp. For neural network training the loss gradient is typically evaluated on a randomly selected subset of the training data and the pure gradient in Eq. 1 is subsequently replaced by a noisy gradient which we denote $\tilde{G}(\theta)$. In the stochastic gradient Langevin dynamics method of [37], the system is further driven by constant variance additive noise. Further, most training procedures incorporate momentum. As a somewhat general model, one may consider a partitioned underdamped Langevin dynamics system of the form:

$$d\theta_\alpha = p_\alpha dt, \quad dp_\alpha = \tilde{G}_\alpha(\theta)dt - \gamma_\alpha p_\alpha dt + \sqrt{2\gamma_\alpha \tau_\alpha} dW_\alpha, \quad \text{where } \alpha = F, S \quad (2)$$

with momentum $p = (p_F, p_S) \in \mathbb{R}^n$ and hyperparameters $\gamma_\alpha, \tau_\alpha > 0$. When evaluating the gradient on the full dataset, Langevin dynamics is provably ergodic [25] and samples from a known distribution. The hyperparameter τ_α controls the driving noise and thus the transition between pure optimization and pure sampling; when small it can benefit neural network optimization [21, 38]. In this paper we will focus on the case $\tau_\alpha = 0$, which corresponds to standard stochastic gradient descent (SGD) with

momentum under re-scaling of the hyperparameters. However, our methods can easily be extended to the more general case or indeed to use other optimizers such as Adam. We have also opted to use the same momentum hyperparameter (γ_α in Eq. 2) for both subsystems to provide a fair comparison with standard SGD with momentum – using different optimizer hyperparameters, as well as exploration of methods which combine different optimizers for different components, is left for future study (see Section 7 and Appendix A). Algorithms can easily be designed based on partitioning into multiple independent components (not just two) evolving at different rates, as we illustrate in Section 3.2.

3 Multirate methods for neural network training

In its most general sense the multirate methods we discuss in this paper involve separating the model parameters (and if applicable, their accompanying momenta variables) Θ into multiple components $\Theta_1, \dots, \Theta_N$ corresponding to different time scales. Slow parameters are updated less frequently than their fast counterparts but with larger step-sizes. Synchronization of the parts occurs every slow time step. This is illustrated for two time-scales (and accompanying fast Θ_F and slow Θ_S parameters) in Figure 2. In this section we discuss application-specific appropriate choices for the fast and slow parameters and propose two specific multirate techniques that can be directly applied to the training of neural networks for classification tasks. The first technique partitions a neural network into fast and slow parts, whereas the second technique puts copies of the same network on different time scales.

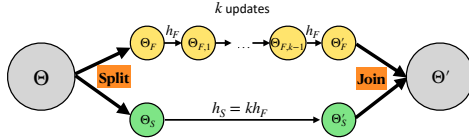


Figure 2: The basic principle of the multirate techniques considered in this paper is illustrated for two time-scales in this figure. We first split our parameters into fast and slow components, Θ_F and Θ_S , respectively. The fast components are then updated every step with step size h_F , whereas the slow components are updated every k steps with step size $h_S = k \cdot h_F$.

3.1 A neural network partition-based multirate approach

The following technique is based on separating the model parameters of a neural network into fast and slow components. Examples of possible separations of the model parameters are layer-wise (which we will use to obtain computational speed-up in a transfer learning context), weights vs. biases, or by selecting (random) subgroups. The appropriate separation is application-specific and will be discussed in more detail in upcoming sections. Although the method can easily be extended to divide the net into N components, as detailed in the supplement, we will focus here and in our experiments on splitting the model into two parts. A multirate algorithm then proceeds as follows:

1. Separate the model parameters into a fast and slow part.
2. Every step: Compute the gradients with respect to the fast variables. Update the fast variables using the optimizer of your choice with fast stepsize h_F .
3. Every $k \in \mathbb{Z}_{>0}$ steps: Compute the gradients with respect to the slow variables. Update the slow variables using the optimizer of your choice using slow step size $h_S = k h_F$.

Below we present our main Algorithm 1. We refer to the model parameters and momenta associated with the slow system as θ_S and p_S , respectively, and for the fast system as θ_F and p_F . We denote $\mathcal{L}(\theta_S, \theta_F)$ as the neural network cross-entropy loss for classification tasks. The base algorithm for our optimization scheme as presented in this paper is stochastic gradient descent (SGD) with momentum, where the gradients are computed for every mini-batch of m training examples. We will compare our multirate approach with PyTorch’s standard SGD with momentum implementation [27] and hence for consistency we present our method in the same notation and manner as used in the PyTorch code. We use μ to denote the momentum hyperparameter, which we typically set to $\mu = 0.9$.

Linear drift. In Algorithm 1 we continuously push the slow parameters along a linear path defined by their corresponding momenta. This means that although the gradients for the slow parameters are only computed every k steps, the slow neural network parameters do get updated every step in the direction of the previous gradient. This is in the vein of the reversible averaging approach to multiple time-stepping [20], but has to our knowledge not been used for multirate techniques before, where Algorithm 2 type approaches are more common. We compare these in ablation studies in Sec. 4.3.

Algorithm 1: Multirate SGD with linear drift

```

 $p_S := \mu p_S + \nabla_{\theta_S} \mathcal{L}(\theta_S, \theta_F)$ 
for  $i = 1, 2, \dots, k$  do
   $p_F := \mu p_F + \nabla_{\theta_F} \mathcal{L}(\theta_S, \theta_F)$ 
   $\theta_F := \theta_F - \frac{h}{k} p_F$ 
   $\theta_S := \theta_S - \frac{h}{k} p_S$ 
end

```

Algorithm 2: Multirate SGD no linear drift

```

 $p_S := \mu p_S + \nabla_{\theta_S} \mathcal{L}(\theta_S, \theta_F)$ 
 $\theta_S := \theta_S - h p_S$ 
for  $i = 1, 2, \dots, k$  do
   $p_F := \mu p_F + \nabla_{\theta_F} \mathcal{L}(\theta_S, \theta_F)$ 
   $\theta_F := \theta_F - \frac{h}{k} p_F$ 
end

```

As extension of this framework to multiple components operating at r scales, one could use stepsizes $h_i = h_{i-1}/K_{i-1}$, $i = 1, 2, \dots, r$, $K_i \in \mathbb{Z}_{>0}$, recursively dividing the step sequences in Algorithm 1 and 2 into finer ones at each successive level of the parameter hierarchy. We discuss other variations of Algorithm 1 such as its combination with Adam, the use of weight decay, or different initializations for the fast/slow systems in Appendix A. In Section 4 we explore obtaining computational speed-up using Algorithm 1 by choosing our fast parameters such that the gradients corresponding to the fast system are quick to compute, while gradients of the full net are only computed every k steps.

3.2 Multirate across neural networks

Our “multi-brain” method is based on the following idea: multiple independent copies (brains) of the same network are trained using different learning rates with their parameters merged whenever two or more copies reach the same time threshold. The copies are trained using an optimizer of the user’s choice, such as SGD or Adam. The goal of our multi-brained approach for neural network training is to detect latent information present at different time scales within the data. This is illustrated for patch-augmented CIFAR-10 data [23] in Figure 1, where our multi-brain approach simultaneously both memorizes the patch and obtains good performance on clean validation data, whereas fixed learning rate approaches fail to do both. To make this more concrete, for two brains the algorithm is:

1. Save two copies of your neural network θ .
2. Train copy 1 for k steps using step-size h_F giving θ_F .
3. Train copy 2 for 1 step using step-size $h_S = k \cdot h_F$ giving θ_S .
4. Update $\theta = (\theta_F + \theta_S)/2$ and go back to step 1.

For a three-brains approach this is visualized in Figure 3. For N -brains, where $h_N = k_{N-1}h_{N-1} = \dots = k_1h_1$ with $k_1 > \dots > k_{N-1} > 1$, $k_{i-1}/k_i \in \mathbb{Z}_{>0} \forall i$ and $h_1 \in \mathbb{R}_{>0}$ as chosen hyperparameters, we present Algorithm 3. We use notation $\mathcal{M}(h_i, \theta_i, p_i, \nabla \mathcal{L}(\theta_i))$ to indicate a standard optimizer step that updates the parameters θ_i and (optionally) accompanying momenta variables p_i of a network using optimization scheme \mathcal{M} , e.g., Adam or SGD, with gradient $\nabla \mathcal{L}(\theta_i)$ and step size h_i .

Algorithm 3: N brains

```

 $\theta = \theta_1 = \dots = \theta_N$ 
for  $i = 1, 2, \dots, m$  do
   $\theta'_1 = \mathcal{M}(h_1, \theta_1, p_1, \nabla \mathcal{L}(\theta_1))$ 
  if  $i \% (k_1/k_2)$  then
     $\theta'_2 = \mathcal{M}(h_2, \theta_2, p_2, \nabla \mathcal{L}(\theta_2))$ 
     $\theta_1 = \theta_2 = (\theta'_1 + \theta'_2)/2$ 
  if  $\dots$  then
    if  $i \% (k_1/k_N)$  then
       $\theta'_N =$ 
         $\mathcal{M}(h_N, \theta_N, p_N, \nabla \mathcal{L}(\theta_N))$ 
       $\theta_1 = \dots = \theta_N =$ 
         $(\theta'_1 + \dots + \theta'_N)/N$ 
end

```

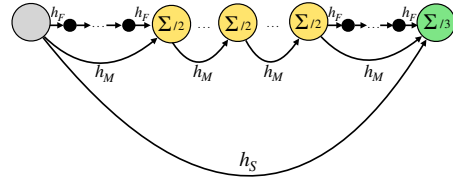


Figure 3: Training with three brains: three copies of the network are trained using different stepsizes $h_S = k_2h_M = k_1h_F$, where h_F, h_M, h_S belong to the fast, medium, and slow time-scales, respectively. When two or more copies have bridged the same time interval, we merge the obtained parameters by averaging the weights of the different copies (indicated by $\Sigma/2$ and $\Sigma/3$ in figure).

4 A multirate approach to transfer learning

We propose a specific layer-wise division of the neural network parameters into fast and slow parts for Algorithm 1, which can be used to significantly speed-up training in a transfer learning context.

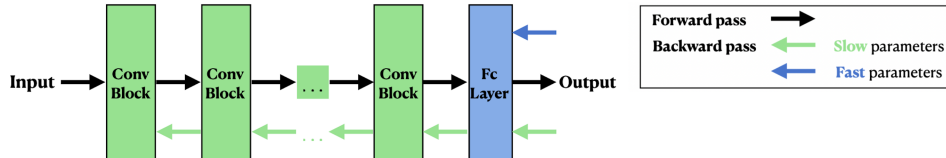


Figure 4: We indicate in blue the fast parameters and in green the slow parameters of a convolutional architecture, which consists of several convolutional blocks (conv block) and fully connected (fc) layer(s). When setting the fast parameters to be the final fc layer(s) (and optionally the conv block directly preceding it), the gradient computation for the backpropagation algorithm is very fast.

The use of pre-trained deep neural networks has become a popular choice of initialization [5, 39]. These pre-trained networks are readily available through popular machine learning libraries, such as PyTorch [27], and are usually trained on large datasets, such as ImageNet for vision applications [15] or large text corpora for natural language processing [14]. Using a pre-trained network as initialization has been shown to significantly speed-up training and typically improves the generalization performance of the resulting model [39, 12, 29]. The procedure is usually: start with a pre-trained model, remove task-specific layers, and then re-train part of the network on the new target task. Later layers of neural networks typically capture more task-specific knowledge, while early layers capture more general features, which can be shared across tasks [39, 10, 26, 30]. Hence to speed up training (and in low target-data scenarios to prevent overfitting), one often does not re-train the full neural network, but only the later layers, in particular the final fully connected layer. This process is called fine-tuning [14, 4]. There exists a delicate balance between computational cost and generalization performance of fine-tuned deep neural network architectures.

We propose to split a neural network into two parts, the fully connected layer parameters –the fast part– and the other parameters of the deep neural network –the slow part. The fast part– is updated with a stepsize h/k , while the other part –the slow part– is only updated every k steps with a stepsize h . The slow part is very large compared to the fast part. For example, for a ResNet34 architecture [11], the fully connected layer parameters (the fast part) only constitutes 0.024% of the total parameters. Because of the way the backpropagation algorithm works, for our fast parameter updates we do not need to compute gradients for the full network, because the fast part is the very last layer of the neural network. This is illustrated schematically in Figure 4. Assuming that computing the gradients constitutes the largest cost of neural network training, we obtain significant speed-up by only needing to compute the full network gradients every k steps. We show that by choosing an appropriate k we can obtain a good generalization performance for nearly half the computational cost.

4.1 Numerical results

We study the computational speed-up and generalization performance of Algorithm 1 compared to standard fine-tuning approaches. We consider a ResNet34 architecture [11], which has been pre-trained on ImageNet [27], to classify CIFAR-10 data [19]. The standard procedure is to first replace the final fully connected layer of the architecture, to be able to match the number of classes of the target dataset, and then to retrain either the full architecture on the target set or only some of the bottom layers (with layer we refer to convolutional blocks in this setting). In contrast our multirate approach only updates the final fully connected (fc) layer every step and updates the rest of the parameters every 5 steps (we have set $k = 5$ in Algorithm 1). Both approaches use as base algorithm SGD with momentum without learning rate decay or weight decay. We use pre-trained ResNet architectures from PyTorch [27] and perform all experiments on NVIDIA DGX-1 GPUs. We compare our approach to different fine-tuning approaches in Fig. 5. Our multirate approach can be used to train the network in almost half the time, without affecting the test accuracy of the resulting net. We show in Fig. 6 that the same observations hold for a pre-trained ResNet50 on CIFAR100 data. We also test our multirate approach on natural language data and consider a pre-trained DistilBERT architecture (obtained from the HuggingFace, transformers library). We fine-tune DistilBERT on SST-2 data [32] and show the computational speed-up and maintained generalization performance obtained using our multirate approach in Fig. 7. Just as for standard fine-tuning approaches, there exists a trade-off between generalization performance and training time. We find that also including the attention block directly preceding the final fully connected layer into the slow parameters further enhances the generalization performance, without significantly increasing the training time.

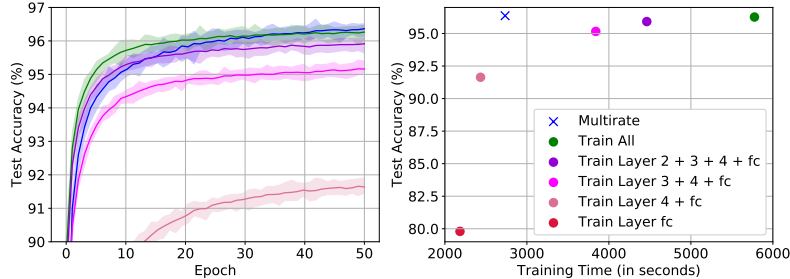


Figure 5: A pre-trained ResNet34 being trained on rescaled CIFAR-10 data using different fine-tuning approaches and our multirate approach (blue). All approaches were trained using SGD with momentum. We set $h/k = 0.001$, $k = 5$, and $\mu = 0.9$ in Algorithm 1. The highest test accuracy is reached using our multirate approach (blue), which can be used to train the net in almost half the time. Typical fine-tuning approaches only train the bottom layers of the network, e.g., layer 4 + fc, which results in a comparable speed-up, but much lower test accuracy. Results are averaged over 20 runs.

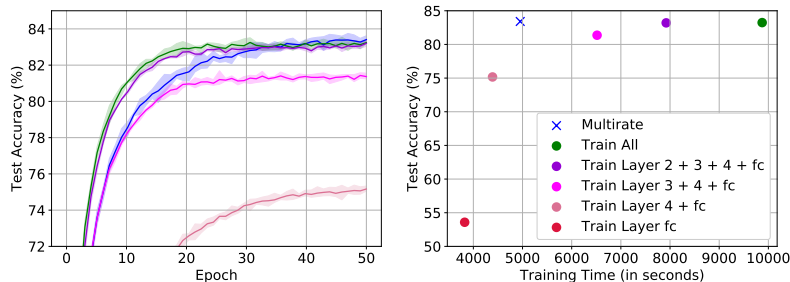


Figure 6: Same set-up as in Fig. 5, but here we consider a pre-trained ResNet50 architecture for rescaled CIFAR-100 data. The highest test accuracy is reached using our multirate approach (blue), which can be used to train the net in almost half the time. Results are averaged over 5 runs.

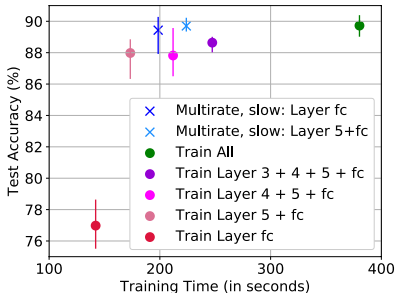


Figure 7: A pre-trained DistilBERT being trained on SST-2 data using different fine-tuning approaches, including our multirate approach (blue). We find that including the final attention block in the slow parameters (together with the fc layer) gives enhanced generalization performance for limited additional cost (light blue) and lowers the variance across multiple runs. We set $h/k = 1e-4$, $k = 5$, and $\mu = 0.9$ in Algorithm 1 and use a batchsize of 16. Results are averaged over 10 runs.

4.2 Complexity analysis

The number of floating point operations (FLOPs) for a forward pass through a neural network forms the lower bound of the execution time [18]. The number of FLOPs required will depend on the architecture and amount of data, whereas the timing of the FLOPs depends on the hardware used [28]. In our case, the number of FLOPs for the forward pass is the same for our multirate algorithm and standard approaches. The speed-up we obtain on ResNet and DistilBERT architectures arises from only needing to compute the gradients for the full net every k steps, while computing the gradients for the final fc layer(s) (and optionally the final convolutional/attention block) of the network every backward pass. The backward pass for the multirate method is hence a subset of the backward pass through the full net. A relevant measure of the speed-up obtained is therefore a ratio of the standard backward pass cost compared to the backward pass cost for our multirate approach over k steps:

$$\frac{\text{backward pass full net}}{\text{backward pass multirate}} = \frac{kL}{L + (k-1)\ell} \quad \text{where } \ell \ll L \quad (3)$$

for a neural network with L layers, where the slow parameters are the final ℓ layers of the network for $\ell \ll L$. When only fine-tuning the last ℓ layers, the L in the numerator is replaced by ℓ , but depending on the choice of ℓ this typically results in a lowered generalization performance. If the number of layers L is large, one can obtain a large speed-up using our multirate approach by only having to backpropagate through the full network every k steps. The exact speed-up obtained depends on the size of the layers and the hardware used. We performed our experiments in PyTorch on NVIDIA DGX-1 GPUs.

4.3 Ablation studies

We consider a pre-trained DistilBERT being fine-tuned on SST-2 using our multirate approach (same set-up as in Fig. 7) and perform ablation studies. We find that pushing the slow parameters along a linear path (as in Algorithm 1) improves the test accuracy compared to Algorithm 2 (Table 1). We also show that using the same step size $h_S = h_F$ for both the fast and slow parameters, but still only updating the slow parameters every k steps, does not lead to the same performance as using larger step size $h_S = k \cdot h_F$ for the slow parameters (Table 2). Finally, we provide a study on the role of k (Table 4 in Appx.) and find optimal performance with $k = 5$, although training time can be decreased by choosing larger values of k . This trade-off needs to be taken into account when choosing k .

Fast params	<i>Linear path?</i>	Mean test acc	Min test acc	Max test acc
Layer fc	Yes	89.43%	87.92%	90.28%
	No	88.69%	87.53%	89.68%
Layer 5 + fc	Yes	89.70%	89.35%	90.23%
	No	89.54%	88.91%	90.44%

Table 1: **Effect of continuously pushing slow parameters along linear path.** Same setting as in Fig. 7, where fast parameters are set to be the fully connected (fc) layer + optionally the final attention block (layer 5) of a DistilBERT. We find that pushing the slow parameters along a linear path during the fast parameter updates improves the mean test accuracy. Results are presented over 10 runs.

Fast params	<i>Higher h for θ_S ?</i>	Mean test acc	Min test acc	Max test acc
Layer fc	Yes	89.43%	87.92%	90.28%
	No	88.78%	87.64%	89.90%
Layer 5 + fc	Yes	89.70%	89.35%	90.23%
	No	89.29%	88.08%	89.95%

Table 2: **Same learning rate for fast and slow parameters.** Same setting as in Fig. 7 for a DistilBERT architecture. We study the effect of using the same learning rate for both the fast and slow parameters, i.e., $h_S = h_F = 1e-4$ vs. using $h_S = k \cdot h_F = 5e-4$. We observe that using a larger learning rate for the slow parameters aids performance. Results are presented over 10 runs.

5 Multirate training from scratch

Whereas the previous section focused on using multirate methods to obtain computational speed-up in transfer learning settings, we will now discuss how multirate methods can be used to enhance the generalization performance of neural networks trained from scratch.

5.1 Using a multirate approach to regularize neural networks

In this section we use randomly selected subsets of the neural network weight matrices (and optionally the biases) to form the slow parameters in Algorithm 1. Every k optimization steps a different subset of the network parameters is randomly selected. For the technique presented here we slightly modify Algorithm 1, by setting all the slow parameters θ_S to be zero during the k fast weight updates. We then re-activate the slow parameters and update them together with the fast weights in a single step with a larger time-step $h \cdot k$ for the slow weights. The base algorithm we use is again SGD and we incorporate our technique directly inside a ready-to-use torch.optimizer. We discuss parallels between our method and dropout in the related work section. We show that this technique can be used to obtain enhanced performance on a single hidden layer perceptron applied to MNIST data in Fig. 8.

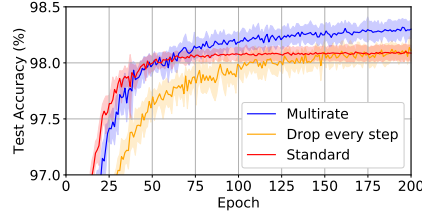


Figure 8: SHLP trained on MNIST using SGD with $h = 0.1$. Our multirate technique (blue) de-activates weights in the input and hidden layer with a probability of 0.8 and 0.5, respectively, and obtains a higher test accuracy than standard SGD (red). We also test removing the multirate component from our approach, which results in an algorithm which sets a different part of the weights to zero every step (orange), and does not perform as well as the multirate technique (blue).

5.2 Multi-brained neural networks

We use the three-brains approach (Algorithm 3) to train a ResNet34 on CIFAR-10 data. In Fig. 3 we show that the method outperforms standard SGD with momentum for any choice of learning rate.

Method	Mean test acc	Min test acc	Max test acc
Three brains $h_F = 0.01, h_M = 0.05, h_S = 0.5$	89.2%	88.1%	90.0%
SGD with mom, $h = 0.05$	86.7%	85.6%	88.1%
SGD with mom, $h = 0.01$	88.7%	87.8%	89.6%
SGD with mom, $h = 0.005$	88.7%	86.9%	89.6%

Table 3: Averaged over 10 runs. A ResNet34 architecture trained on CIFAR-10 data with SGD with momentum, weight decay, and different stepsizes. The three brains approach outperforms all.

6 Related Work

Intuition for using fast/slow weights in a machine learning context can be found in neuroscience, as synapses have dynamics at different time-scales. One of the earliest mentions of fast and slow weights in the machine learning literature was by Hinton and Plaut (1987) [13], who set each connection to have both a fast-changing weight, which was supposed to act as a temporary memory, and a slowly-changing weight which stored long-term knowledge. More recently, Ba et al. (2016) [1] used fast weights as a temporary memory to improve recurrent neural networks. Further, our multirate approach to transfer learning (Sec. 4) has similarities to multiple time-stepping techniques used in molecular dynamics, such as r-RESPA [34, 35], where the fast dynamics is typically cheap to compute in comparison with the slow dynamics. This is similar to our transfer learning application, where we set the final layer of the net to be the fast part to obtain computational speed-up. Further inspiration arises from the use of partitioned integrators for neural network training. It is well-known that different layers play different roles [42] and that later layers capture more task-specific knowledge, while early layers capture more general features, which can be shared across tasks [39, 10, 26, 30]. It is hence natural to train the different layers of the neural network using layer-wise adaptive learning rates [40], layer-wise large-batch optimization techniques [41], or using different optimizers [21].

The multirate regularization technique (Sec. 5.1) has similarities to Dropout [33] and DropConnect [36]. Dropout can enhance the robustness and generalization performance of neural networks, and is used widely, although its performance in combination with batch normalization [16] is an ongoing area of research [24, 22, 2]. In contrast to dropout and its variants we do not modify the network architecture but incorporate our technique inside the optimizer, which randomly selects a subset of the weights as the slow part and keeps these de-activated for multiple steps. These weights are then re-activated and updated with a larger time-step, before de-activating a different subset. In this work we merely aim to illustrate the potential of using multirate techniques as a manner of regularization, but see an exploration of multirate variants of dropout as an exciting avenue for future work.

Finally, our multi-brain approach (Sec. 3.2) has similarities with stochastic weight averaging (SWA) [17]. In the SWA method one averages the weights sampled from a set of neural network models at later stages of training using SGD with a modified learning rate schedule. This achieves enhanced generalization performance for pre-trained models. In contrast to SWA, we use our multi-brain approach to train networks from scratch and use fixed learning rates to train the different copies of the networks. We also have one less hyperparameter to tune, as the cycle length c of when weight

averaging takes place is in our case defined by the ratio h_S/h_F . Similar to SWA, our approach is straightforward to implement, has almost no computational overhead compared to standard SGD (only cost is computing the weight average and storing one or multiple copies of the model in memory), and leads to enhanced generalization performance compared to fixed learning rate schedules.

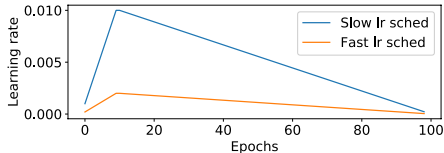
7 Discussion and future work

We outline possible directions for future work using multirate methods for neural network training along three axes: different splitting choices of the neural network parameters into fast and slow parts, use of different optimizers or optimizer hyperparameters to train the different partitions, and further generalizations of the methods by combining them with well-known machine learning techniques.

Different splitting choices. Multirate Algorithm 1 was based on a separation of the neural network parameters into fast and slow parts. We illustrated the potential of this approach for two different parameters splittings: 1) Layer-wise, where we set the final layer(s) to be the fast parameters and the remaining parameters to be the slow parameters (Sec. 4). 2) Random subgroups, where we randomly selected a different subset of the network parameters to be the slow parameters every k optimization steps (Sec. 5.1). An interesting direction for future work is to further explore layer-wise splitting when training networks from scratch, e.g., one could separate the early from later layers and train these with different timescales. This may benefit training as layers have different sensitivities to re-initialization [42] and layer-wise adaptive learning rates can aid training [40]. Another option is to set the biases of a MLP architecture to be the slow parameters, while keeping the weights on the fast time-scale. In Appx. C we show that using this approach we can obtain much higher test accuracies on spiral data and provide ablation studies. This illustrates the potential of other parameter splittings.

Hybrid optimization schemes. For our multirate approach we partition the network into multiple parts which we train on different timescales. A natural extension is to also use different optimizers or optimizer hyperparameters to train the different partitions, e.g., using SGD for the slow part, but SGD with momentum for the fast part(s), or using sampling techniques such as SGLD or discretized Langevin dynamics for a part that requires more exploration. In this work we focused on using the same base algorithm for all partitions to keep the focus on the role of different timescales. However, we expect that using hybrid optimization schemes may lead to further performance enhancement.

Further generalizations. Since our multirate approaches act as an add-on to standard optimization schemes, they can be applied in combination with other machine learning techniques. As a simple illustration consider a slanted triangular learning rate schedule [14]. By training two networks simultaneously using two different maximum learning rates one can obtain a small performance enhancement on the test data (Fig. 9). This serves as an illustration that multirate approaches can be easily combined with existing techniques and can improve performance. Another interesting direction for future work is a multirate variant of dropout as discussed in the related work section.



Method	Test accuracy
Adam $h_{max} = 0.002$	91.76 \pm 0.24%
Adam $h_{max} = 0.01$	91.55 \pm 0.48%
Multirate	91.88 \pm 0.12%

Figure 9: A ResNet34 architecture trained on CIFAR-10 data using Adam with a slanted triangular learning rate schedule (lr sched) [14], where we increase the learning rate from $h_0 = h_{max}/32$ to h_{max} in the first 10 epochs. A weight averaging multirate approach with base algorithm Adam (lr sched shown left) obtains a higher test accuracy avg. over 10 runs. Further details in Appendix B.

Conclusion. Our results illustrate the potential of multirate methods for various neural network training applications, such as transfer learning, regularization, and weight averaging. Our methods act as an add-on to standard optimizers so (although we focused on SGD in this paper) they can easily be applied in combination with other optimizers. By introducing the use of multirate techniques to the machine learning community, showing their use in different training settings, and outlining various directions for future work, we hope to have built a strong foundation for further research in this area.

References

- [1] J. Ba, G. Hinton, V. Mnih, J. Z. Leibo, and C. Ionescu. Using fast weights to attend to the recent past. *NeurIPS*, 2016.
- [2] G. Chen, P. Chen, Y. Shi, C. Hsieh, B. Liao, and S. Zhang. Rethinking the usage of batch normalization and dropout in the training of deep neural networks. *arXiv:1905.05928*, 2019.
- [3] E.M. Constantinescu and A. Sandu. Extrapolated multirate methods for differential equations with multiple time scales. *Journal of Scientific Computing*, 56(1):28–44, 2013.
- [4] A.M. Dai and Q.V. Le. Semi-supervised sequence learning. *NIPS*, 2015.
- [5] J. Devlin, M.-W. Chang, K. Lee, and K. Toutanova. BERT: Pre-training of deep bidirectional transformers for language understanding. *arXiv preprint arXiv:1810.04805*, 2018.
- [6] Ch. Engstler and Ch. Lubich. Multirate extrapolation methods for differential equations with different time scales. *Computing*, 58:173–185, 1997.
- [7] C. W. Gear. Multirate methods for ordinary differential equations. *Technical Report, University of Illinois*, 1974.
- [8] C.W. Gear and D.R. Wells. Multirate linear multistep methods. *BIT*, 24:484–502, 1984.
- [9] M. Günther and P. Rentrop. Multirate row methods and latency of electric circuits. *Appl. Numer. Math.*, 13:83–102, 1993.
- [10] Y. Hao, L. Dong, F. Wei, and K. Xu. Visualizing and understanding the effectiveness of BERT. *EMNLP*, 2019.
- [11] K. He, X. Zhang, S. Ren, and J. Sun. Deep residual learning for image recognition. In *Proceedings of the IEEE conference on computer vision and pattern recognition*, pages 770–778, 2016.
- [12] K. He, R. Girshick, and P. Dollár. Rethinking ImageNet pre-training. *ICCV*, 2019.
- [13] G. E. Hinton and D. C. Plaut. Using fast weights to deblur old memories. In *Proceedings of the ninth annual conference of the Cognitive Science Society*, pages 177–186, 1987.
- [14] J. Howard and S Ruder. Universal language model fine-tuning for text classification. *ACL*, 2018.
- [15] M. Huh, P. Agrawal, and A. A. Efros. What makes ImageNet good for transfer learning? *arXiv:1608.08614*, 2016.
- [16] S. Ioffe and C. Szegedy. Batch normalization: Accelerating deep network training by reducing internal covariate shift. *ICML*, 2015.
- [17] P. Izmailov, D. Podoprikin, T. Garipov, D. Vetrov, and A. G. Wilson. Averaging weights leads to wider optima and better generalization. *Uncertainty in Artificial Intelligence*, 2018.
- [18] D. Justus, J. Brennan, S. Bonner, and A.S. McGough. Predicting the computational cost of deep learning models. *CoRR*, 2018.
- [19] A. Krizhevsky and G. Hinton. Learning multiple layers of features from tiny images. 2009.
- [20] B. Leimkuhler and S. Reich. A reversible averaging integrator for multiple time- scale dynamics. *Journal of Computational Physics*, 171(1):95–114, 2001.
- [21] B. Leimkuhler, C. Matthews, and T. Vlaar. Partitioned integrators for thermodynamic parameterization of neural networks. *Foundations of Data Science*, 1(4):457–489, 2019.
- [22] X. Li, S. Chen, X. Hu, and J. Yang. Understanding the disharmony between dropout and batch normalization by variance shift. *IEEE/CVF Conference on Computer Vision and Pattern Recognition*, 2019.

- [23] Y. Li, C. Wei, and T. Ma. Towards explaining the regularization effect of initial large learning rate in training neural networks. *NeurIPS*, 2019.
- [24] P. Luo, X. Wang, W. Shao, and Z. Pen. Towards understanding regularization in batch normalization. *ICLR*, 2019.
- [25] J.C. Mattingly, A.M. Stuart, and D.J. Higham. Ergodicity for SDEs and approximations: locally Lipschitz vector fields and degenerate noise. *Stochastic Processes and their Applications*, 101(2):185–232, 2002.
- [26] B. Neyshabur, H. Sedghi, and C. Zhang. What is being transferred in transfer learning? *NeurIPS*, 2020.
- [27] A. Paszke, S. Gross, S. Chintala, G. Chanan, E. Yang, Z. DeVito, Z. Lin, A. Desmaison, L. Antiga, and A. Lerer. Automatic differentiation in PyTorch. 2017.
- [28] H. Qi, E. R. Sparks, and A. Talwalkar. PALEO: A performance model for deep neural networks. *ICLR*, 2017.
- [29] A. Radford, K. Narasimhan, T. Salimans, and I. Sutskever. Improving language understanding by generative pre-training. *OpenAI*, 2018.
- [30] M. Raghu, C. Zhang, J. Kleinberg, and S. Bengio. Transfusion: Understanding transfer learning for medical imaging. *NeurIPS*, 2019.
- [31] J. R. Rice. Split runge-kutta methods for simultaneous equations. *Journal of Research of the National Institute of Standards and Technology*, 60, 1960.
- [32] R. Socher, A. Perelygin, J. Wu, J. Chuang, C. Manning, A. Ng, and C. Potts. Recursive deep models for semantic compositionality over a sentiment treebank. *Conference on Empirical Methods in Natural Language Processing*, 2013.
- [33] N. Srivastava, G. Hinton, A. Krizhevsky, I. Sutskever, and R. Salakhutdinov. Dropout: a simple way to prevent neural networks from overfitting. *JMLR*, 15:1929–1958, 2014.
- [34] M. E. Tuckerman, B. J. Berne, and G. J. Martyna. Molecular dynamics algorithm for multiple time scales: Systems with long range forces. *The Journal of Chemical Physics*, 94(10):6811–6815, 1991.
- [35] M. E. Tuckerman, B. J. Berne, and G. J. Martyna. Reversible multiple time scale molecular dynamics. *The Journal of Chemical Physics*, 97(3):1990–2001, 1992.
- [36] L. Wan, M. Zeiler, S. Zhang, Y. Le Cun, and R. Fergus. Regularization of neural networks using DropConnect. *ICML*, 2013.
- [37] M. Welling and Y. W. Teh. Bayesian learning via stochastic gradient Langevin dynamics. In *Proceedings of the 28th International Conference on Machine Learning (ICML-11)*, pages 681–688, 2011.
- [38] F. Wenzel, K. Roth, B. S. Veeling, J. Swiatkowski, L. Tran, S. Mandt, J. Snoek, T. Salimans, R. Jenatton, and S. Nowozin. How good is the Bayes posterior in deep neural networks really? *arXiv:2002.02405*, 2020.
- [39] J. Yosinski, J. Clune, Y. Bengio, and H. Lipson. How transferable are features in deep neural networks? *NIPS*, 2014.
- [40] Y. You, I. Gitman, and B. Ginsburg. Large batch training of convolutional networks. *arXiv preprint arXiv:1708.03888*, 2017.
- [41] Y. You, J. Li, S. Reddi, J. Hseu, S. Kumar, S. Bhojanapalli, X. Song, J. Demmel, K. Keutzer, and C. Hsieh. Large batch optimization for deep learning: training BERT in 76 minutes. *ICLR*, 2020.
- [42] C. Zhang, S. Bengio, and Y. Singer. Are all layers created equal? *arXiv:1902.01996*, 2019.

A Variants of our multirate training algorithms

Our multirate training schemes either partition the network parameters into multiple components (Algorithm 1 and 2) or place multiple copies of the same network on multiple time scales (Algorithm 3). Either of these settings lends themselves naturally to training the different components (or copies) using different optimization strategies.

To discuss this more concretely, recall Langevin dynamics from Eq. 2 in the main paper:

$$\begin{aligned} d\theta_\alpha &= p_\alpha dt, \\ dp_\alpha &= \tilde{G}_\alpha(\theta)dt - \gamma_\alpha p_\alpha dt + \sqrt{2\gamma_\alpha\tau_\alpha} dW_\alpha, \text{ where } \alpha = F, S, \end{aligned}$$

with neural network parameters $\theta = (\theta_F, \theta_S) \in \mathbb{R}^n$, momentum $p = (p_F, p_S) \in \mathbb{R}^n$, noisy (due to subsampling) gradient $\tilde{G}_\alpha(\theta)$ of the loss with respect to θ_α , Wiener process W , and hyperparameters $\gamma_\alpha, \tau_\alpha > 0$. Using discretized Langevin dynamics to train neural networks allows for incorporation of both momentum and additive noise, the size of which is controlled by the γ_α and τ_α hyperparameters, respectively. A straightforward variant is thus to use different values for γ_α and/or τ_α for the fast and slow components. Hyperparameter τ controls the transition between a pure optimization and sampling approach and when small can benefit neural network optimization [21, 38]. Using small values of τ for parts of the dynamics that require further exploration may thus benefit training. On the other hand, to train a component with stochastic gradient descent with momentum one can set $\tau = 0$. An example of a possible combination of Langevin dynamics with additive noise for the fast dynamics and without additive noise (corresponding to SGD) for the slow dynamics is then:

$$\begin{aligned} d\theta_F &= p_F dt, \quad dp_F = \tilde{G}_F(\theta)dt - \gamma_F p_F dt + \sqrt{2\gamma_F\tau} dW_F \\ d\theta_S &= p_S dt, \quad dp_S = \tilde{G}_S(\theta)dt - \gamma_S p_S dt. \end{aligned}$$

Equivalently, one could change the value of the momentum hyperparameter γ_α for the different partitionings. Or use different optimizers for the different components, such as Adam and SGD. Finally, it would be interesting to study the effect of using different size initializations for the different components, which essentially starts off the different components on different scales. Of course, any of these suggestions require extra tuning of the algorithm, which is why we focused on SGD with the same momenta values and initializations for all components in the paper. We expect however that using hybrid optimization schemes may lead to even further performance enhancement, which we aim to explore in future work. Further, the effect of using Adam or AdamW as base algorithm (instead of SGD with momentum) for Algorithm 1 and 3 would be interesting to explore. Other optimizers can be easily combined with our approaches (as illustrated for Adam in Figure 9).

As a simple extension of Algorithm 1 we provide the case with weight decay in Algorithm A4, where we have used ω to denote the amount of weight decay. Our implementation of weight decay is the same as used in PyTorch for SGD [27]. We did not use weight decay for our experiments in the paper.

Algorithm A 4: Multirate SGD with linear drift and weight decay

```

 $p_S := \mu p_S + \nabla_{\theta_S} \mathcal{L}(\theta_S, \theta_F) + \omega_S \theta_S$ 
for  $i = 1, 2, \dots, k$  do
     $p_F := \mu p_F + \nabla_{\theta_F} \mathcal{L}(\theta_S, \theta_F) + \omega_F \theta_F$ 
     $\theta_F := \theta_F - \frac{h}{k} p_F$ 
     $\theta_S := \theta_S - \frac{h}{k} p_S$ 
end

```

B Further experimental details

We run our experiments (unless indicated otherwise) with SGD with momentum set to 0.9. The learning rate varied per experiment and is detailed in the captions of the figures. For the transfer learning experiments (Section 4) it was set to $h = 0.001$ for the ResNet architectures and to $h = 1e-4$ for the DistilBERT and we did not use weight decay. In Algorithm 1 we set $k = 5$ and varied our partitionings of the network parameters into fast and slow parts. In Algorithm 3 we chose the step sizes, which then automatically determined the values for the k_i ; the momenta were not re-set, but

carried along throughout training to take advantage of the history information. All our experiments were run in PyTorch using NVIDIA GPUs.

We will discuss specific experiments that require further details below.

B.1 Patch-augmented CIFAR-10

The patch-augmented CIFAR-10 dataset that we used for Figure 1 was adapted from the paper by Li et al. (2019) [23]. We first split the 50000 CIFAR-10 training images, into 10000 patch-free images and 40000 images which contain only a patch with probability 0.2 and contain a patch mixed with CIFAR-10 data with probability 0.8. The 7×7 pixel patch is located in the center of the images. Following Li et al. (2019) [23] to generate the patch, we first sample $z \sim \mathcal{N}(0, 1.5625)$, a a random float in $[0,1)$, and $\zeta_i \sim [-0.1, 0.1]$ for classes $i = 1, \dots, 10$. Then for patch-only images belonging to class i we set everything to 0 and add $z \pm 1.75a\zeta_i$. To generate images containing both a patch and CIFAR-10 data we add $z \pm \zeta_i$.

B.2 Triangular learning rate

For the triangular learning rate experiment presented in Figure 9 of the main paper, we first define a maximum learning rate value h_{max} . Then we linearly increase the learning rate from $h_{max}/32$ to h_{max} in the first 10 epochs. The learning rate then linearly decreases to zero in the next 90 epochs. For the multirate approach we have two separate learning rate schedules with distinct $h_{max,i}, i = F, S$ which we use to train two separate copies of the network using Adam. We average the weights obtained every k steps in the vein of Algorithm 3. In contrast to our Algorithm 3 however the averaging of the weights does not occur when the same time-scale has been bridged, because this would be difficult to achieve due to the ever changing learning rate values. Therefore, the value of k is an additional hyperparameter for this example, whereas in our other multi-brain experiments k is defined by the ratio of the step sizes for fast/slow systems. We set $h_{max,S} = 0.01$, $h_{max,F} = 0.002$, and $k = 10$ to obtain Figure 9.

C Slow biases

We study the effect of putting all the biases of a neural network on the slow time-scale, while keeping the weights on the fast time-scale and only updating the slow parameters every k steps using Algorithm 1. Surprisingly, this gives big performance improvements on 4-turn spiral data (adapted from [21]) as shown in Figure A10. Figure A11 confirms that this enhanced performance is caused by our multirate technique, i.e., freezing the biases for k steps and then boosting them with a larger time-step. Simply putting the biases on a different time-scale or freezing the biases for k steps and using the same time-step does not lead to the same performance improvement. In Figure A12 we show that this effect is caused by the input layer biases, in particular. This seems to suggest a possible connection with data normalization (and the lack thereof for the spiral dataset). In Figure A13 we show that for a ResNet-34 architecture on CIFAR-10 data one also obtains a small performance improvement by using slow biases for the fully connected layer, especially when no data augmentation is used.

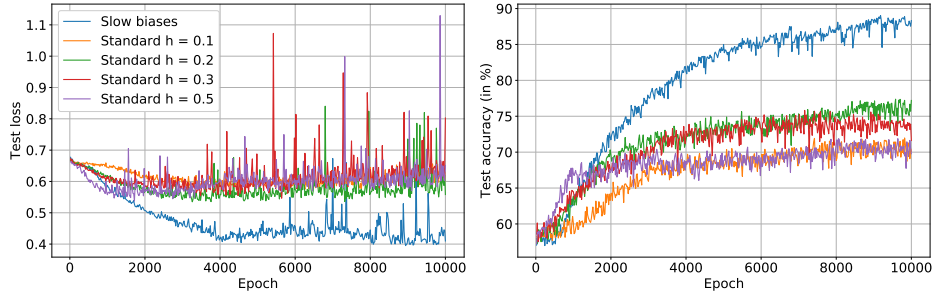


Figure A10: We use both standard SGD and our multirate approach as defined in Algorithm 1 to train a SHLP on a 4-turn spiral problem with 5% subsampling. We set the biases of the neural network to be θ_S and the weights to be θ_F and set $k = 5$, $h = 1$ in Algorithm 1. Results are averaged over 5 runs.

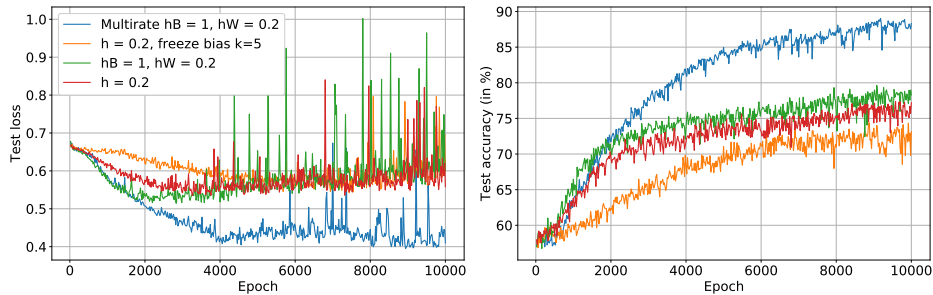


Figure A11: Same setting as in Figure A10, with a SHLP being trained on spiral data using SGD with $h = 0.2$ (red). We show that putting the biases on a different time-scale (green) or freezing the biases for $k = 5$ steps and then updating them with the same step size as for the fast (weight) parameters (orange) both do not lead to the same performance improvement as our multirate technique (blue).

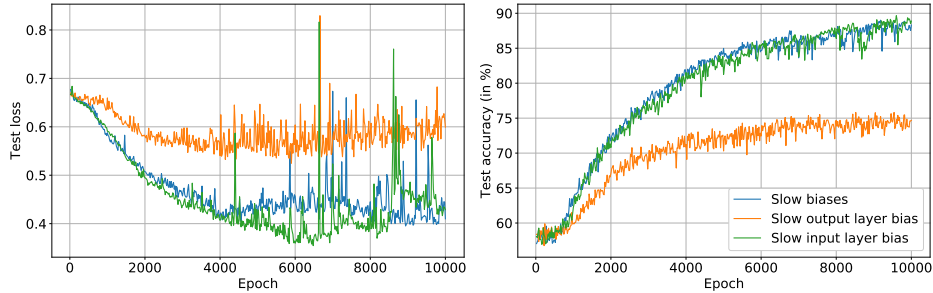


Figure A12: Same setting as in Figure A10, but here we study the effect of only putting the input biases (green) or only the output biases (orange) on the slow time-scale. Clearly, using slow input biases (green) appears to be key to the enhanced generalization performance of the multirate approach (blue) in this setting.

D Further ablation studies

The effect of k is studied in Table A4 for fine-tuning a pre-trained DistilBERT on SST-2 data using Algorithm 1. We find that although smaller values of k can improve the generalization performance, the training time gets increased. This trade-off needs to be taken into account when choosing k . Apart from this, recall that lower values of k also lower the step size used for the slow parameters, which can affect performance. As a rule of thumb, we found that setting $k = 5$ gives enough speed-up, without affecting the accuracy.

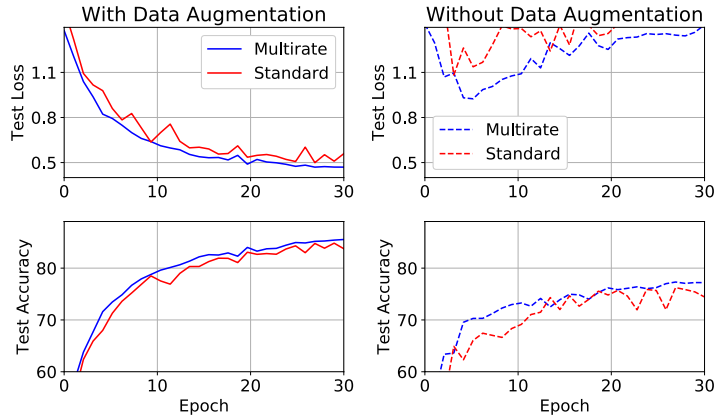


Figure A13: We use both standard SGD (with $h = 0.1$) and our multirate approach as defined in Algorithm 1 to train a ResNet34 architecture on CIFAR-10 data. We set the biases of the fully connected layer of the neural network to be θ_S and the weights to be θ_F and set $k = 10$, $h = 1$ in Algorithm 1 and use $\text{batchsize} = 128$. Results are averaged over 10 runs.

Fast params	k	Mean test acc	Min test acc	Max test acc	Avg Time (s)
Layer fc	$k = 3$	89.26%	88.69%	90.01%	245
	$k = 5$	89.43%	87.92%	90.28%	198
	$k = 10$	88.53%	84.79%	89.79%	180
Layer 5 + fc	$k = 3$	88.91%	87.42%	90.06%	264
	$k = 5$	89.70%	89.35%	90.23%	224
	$k = 10$	88.65%	87.97%	89.73%	207

Table A4: **Effect of k .** A pre-trained DistilBERT being trained on SST-2 data using our multirate approach for different values of k (same setting as in Figure 7), where the fast parameters are set to be the fully connected (fc) layer + optionally the final attention block (layer 5). We set $h/k = 1e-4$ and $\mu = 0.9$ in Algorithm 1 and use a $\text{batchsize} = 16$. Results are presented over 10 runs.